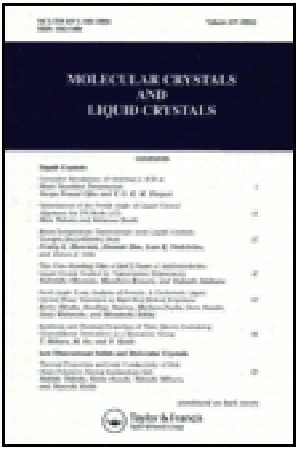

Molecular Crystals and Liquid Crystals Science and Technology. Section A. Molecular Crystals and Liquid Crystals

Publication details, including instructions for authors and subscription information:
http://www.tandfonline.com/loi/gmcl19

Characterization of (Perfluorodecyl) n-Alkanes, $F(CF_2)_{10}(CH_2)_mH$

Shigeru Mita [a], Masakazu Fujiwara [a] & Shoichi Kondo [a]

[a] Department of Chemistry, Faculty of Science, Science University of Tokyo, Kagurazaka, Shinjuku-ku, Tokyo, 162-8601, JAPAN

Version of record first published: 24 Sep 2006

To cite this article: Shigeru Mita, Masakazu Fujiwara & Shoichi Kondo (1999): Characterization of (Perfluorodecyl) n-Alkanes, $F(CF_2)_{10}(CH_2)_mH$, Molecular Crystals and Liquid Crystals Science and Technology. Section A. Molecular Crystals and Liquid Crystals, 330:1, 37-44

To link to this article: http://dx.doi.org/10.1080/10587259908025574

Mol. Cryst. Liq. Cryst., 1999, Vol. 330, pp. 37-44
Reprints available directly from the publisher
Photocopying permitted by license only

Characterization of (Perfluorodecyl) *n*-Alkanes, $F(CF_2)_{10}(CH_2)_mH$

SHIGERU MITA, MASAKAZU FUJIWARA and SHOICHI KONDO

Department of Chemistry, Faculty of Science, Science University of Tokyo,
Kagurazaka, Shinjuku-ku, Tokyo 162–8601 JAPAN

A homologous series of semifluorinated *n*-alkanes, F $(CF_2)_{10}(CH_2)_m$ H, with $2 \leq m \leq 19$ has been synthesized and their properties characterized using a polarising microscope, differential scanning calorimetry and X-ray diffraction. The compounds of $6 \leq m \leq 12$ exhibit the smectic B phase. The molecules from $m = 13$ to 19 show only a melting endotherm in the DSC traces. Conformational structured are discussed on the basis of *ab initio* calculations.

Keywords: mesophase; semifluorinated alkane; smectic B phase

INTRODUCTION

Unlike *n*-alkanes, semifluorinated *n*-alkanes have generated considerable interest due to their unique structures in liquid crystalline compounds. The liquid crystalline compounds usually have a mesogen of core rings. The fluorocarbon segment is actually a rigid linear rod adopting a helical structure due to the intramolecular steric repulsion of the fluorines along the carbon backbone. The possibility of liquid crystalline behavior in the molecules is due to the fluorinated segment acting as the mesogenic unit. A variety of techniques have been used to study the structure of these compounds and a significant number of papers has been published on their structure in the mesophase, the solid phase and in solution.

A comprehensive study and a detailed description of the transition behavior have been presented for $F(CF_2)_{12}(CH_2)_mH$[1, 2, 3, 4]. The structures for an isolated chain and the possible packing in the crystal lattice have also been studied using semi-empirical and molecular field methods[4]. On the other hand, a series of $F(CF_2)_{10}(CH_2)_mH$, abbreviated as F10H*m*, has been studied concerning the dielectric behavior[5] and the layer structure mainly for F10H10 [6, 7, 8]. In this paper, we will present additional data concerning the thermal behavior and lamella structure for fluorocarbon molecules of ten carbon atoms bonded to a hydrocarbon with a different carbon number.

EXPERIMENTAL

The semifluorinated *n*-alkanes of $m = 2, 5$ and $m = 6 \sim 19$ were synthesized using the method of Möller *et al.*[1] and Rabolt *et al.*[3], respectively. These materials were purified by several recrystallizations from methanol/acetone and by Kugelrohr distillations to give the product as a white powder. The final products were determined to be > 99% pure by gas chromatographic analysis.

Optical micrographs were recorded using an OLYMPUS BH-2 polarizing microscope equipped with a Mettler FP82 hot stage and FP80 central processor. Differential scanning calorimetry measurements were performed on a Mettler TA3000 apparatus at a constant heating/cooling rate of 1K/min. X-ray diffraction patterns were obtained using a RIGAKU RINT2100.

The geometries at the minimum energy of F10H*m* were determined from *ab initio* electronic structure calculations using a 4-31G basis set in the Gaussian 94 program.

RESULTS AND DISCUSSION

Figure 1 shows the variation in the transition temperature with respect to the length of the hydrocarbon segment for all the compounds studied. The temperatures for $m = 10$ are in fair agreement with the reported values[6, 7]. The transition behavior of the compounds except for $m = 6$

depends on the thermal history of the sample. The clearing temperatures increase with increasing carbon number of the hydrogen segment. The compounds ranging from $m = 6$ to 12 in hydrogenated carbon atoms are found to exhibit mesophases. These compounds show irregularity in the transition temperatures from a lower temperature phase (P_2) to a higher one (P_1). This would suggest a different structure in the P_2 phase or a different disorder in the hydrocarbon segment.

Figure 2 shows the change in entropy at the clearing temperature and also at the transition temperature from the P_2 to the P_1 phase. The entropy change at the clearing point significantly increases with the number of methylene units in the hydrocarbon segment, while that at the P_2 to the P_1 transition is almost independent of the number of methylene units. Contrary to F10Hm, the hydrocarbon length dependency of these entropy changes was reversed for F12Hm[1] in which the entropy change at the melting point was independent of the hydrocarbon number. The value of entropy change at the P_2 to P_1 transition for F10H10 is clearly out of the line with the other points and is extremely small. This finding implies that at least an additional transition should exist at a temperature lower than this temperature.

The polarization microscopic texture of the P_1 phase for F10H7 is shown in Fig. 3(a). The mosaic texture and the homeotropic black are more likely to be the characteristic texture of the smectic B phase than the other smectic phases. The black field in the texture is due to the orientation of molecules perpendicular to the glass. The black areas turn bright when the sample is tilted or sheared. Figure 3(b) shows the texture of the P_2 phase in which the main domain remains unchanged and vertical lines appear in the domain. It is difficult to identify the phase based on only these observations.

Figure 4 shows the X-ray diffraction patterns at various temperatures for F10H7. Sharp scattering consisting of the first to third orders in the P_1 phase indicates that the molecules are arranged in well-developed layers. For the P_2 phase, it is difficult to rule out the possibility of a crystalline phase from the appearance of several reflections in the small angle region

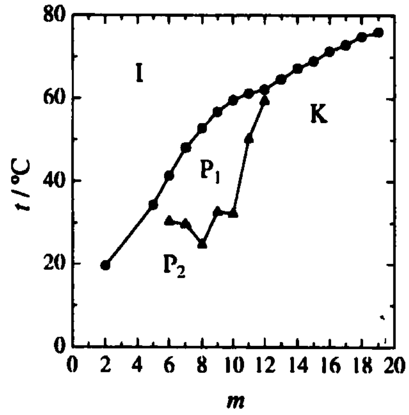

FIGURE 1 Plots of the phase transition temperature as a function of carbon number m of the hydrocarbon segment for F10Hm. I:isotropic. P_1 and P_2: mesophase. K: crystal.

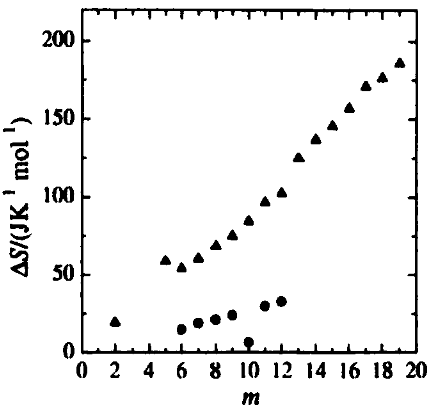

FIGURE 2 Entropy changes at the clearing temperature (▲) and at the P_1 to P_2 phase transition temperature (●) for F10Hm.

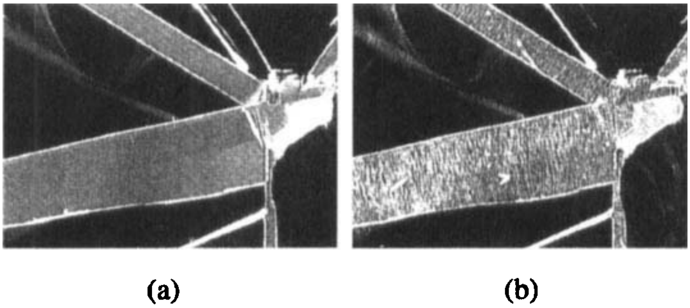

FIGURE 3 Optical texture of F10H7. Crossed polarizers. (a)47.8 °C and (b)27.7 °C, first cooling. x100.

as well as in the wide-angle region.

Figure 5 shows the temperature dependence of the layer spacing for F10H*m*, $m = 6$ to 10. The layer spacing (d_{P_l}) in P_l and the molecular length ($L_{cal.}$) calculated from *ab initio*(HF/4-31G) are given in Table I. As for the conformation, the molecule consists of a planar zigzag hydrocarbon segment joined to a helical fluorinated carbon segment. The molecular length of F10H*m*, ($m = 6 \sim 10$) is smaller than the layer spacing, where the molecular length was defined as the distance between the centers of the terminal fluorine and hydrogen atoms. These small differences correspond

TABLE I The layer spacing in P_l phase and calculated molecular length of F10H*m*.

m	d_{P_l} / nm	$L_{cal.}$ / nm	Δd / nm [1]
6	2.248	2.113	0.135
7	2.381	2.242	0.139
8	2.508	2.369	0.139
9	2.624	2.498	0.126
10	2.752	2.624	0.128

1):$\Delta d = d_{P_l} - L_{cal.}$.

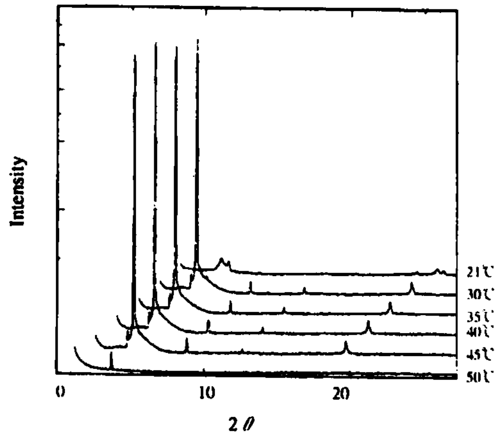

FIGURE 4 WAXD profiles of F10H7 at various temperatures.

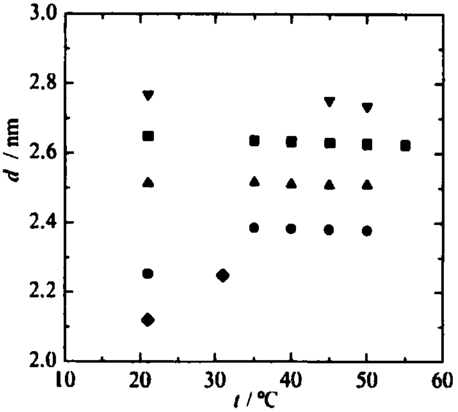

FIGURE 5 Temperature dependence of layer spacing of F10H6(◆), F10H7(●), F10H8(▲), F10H9(■) and F10H10(▼).

to the van der Waals radius of the terminal atoms[9]. Figure 6 illustrated the molecular model of F10H7 at the minimum energy state based on *ab initio* calculations. The carbon atoms of the fluorinated sequence are numbered from the terminal atom. The torsional angles are 17.4° and 11.4° for $\phi(C_1C_2C_3C_4)$ of the terminal part and $\phi(C_9C_{10}CH_2CH_2)$ of the central part, respectively. The other torsional angles of the helical fluorinated carbon segment are $18.6 \pm 0.1°$, which is essentially consistent with 18.1° for perfluorohexane[10]. The P_1 phase is identified as the smectic B phase by the fact that the layer spacing is close to the calculated molecular length, and a sharp wide-angle reflection in the X-ray diffraction and the texture characteristic of the smectic B in the microscope are revealed.

In the cases of F10H7 and F10H9, two different layer spacings are found in the P_2 phase. Both layer spacings are smaller than that in the P_1. In this phase, the molecular long axes are not perpendicular to the layer plane. The tilt angles of F10H7 and F10H9 in the P_2 phase are estimated to be 26.4° and 25.8°, respectively.

FIGURE 6 The molecular model at the minimum energy calculated by *ab initio* for F10H7.

CONCLUSIONS

The presence of the smectic B phase is found when the number of methylene unit is in the range of $m = 6$ to 12. When the hydrocarbon segment is longer than $m = 13$, there is only the melting point because the rigid sequence of the fluorocarbon helix compared with the considerable mobility of the hydrocarbon sequence is too short to establish such a mesophase. For $m = 2$ and 5, no evidence is found for the formation of a mesophase.

The change in entropy at the clearing temperature significantly depends on the length of hydrocarbon segments.

Acknowledgments

We cordially thank Dr. S. Ujiie (Shimane University) for the X-ray diffraction measurements.

References

[1] J. Höpken, C. Pugh, W. Richtering, and M. Möller, *Makromol. Chem.*, **189,** 911 (1988).
[2] J. Höpken and M. Möller, *Macromolecules,* **25,** 2482 (1992).
[3] J.F. Rabolt, T.P. Russell, and R.J. Twieg. *Macromolecules,* **17,** 2786 (1984).
[4] T.P. Russell. J.F. Rabolt. R.J. Twieg, R.L. Siemens, and B. L. Farmer, *Macromolecules,* **19,** 1135 (1986).
[5] K. Araki, K. Satoh, and S. Kondo, *Mol. Cryst. Liq. Cryst.* **302,** 369 (1997).
[6] W. Mahler, D. Guillon. and A. Skoulios. *Mol. Cryst. Liq. Cryst Letters,* **2,** 111 (1985).
[7] C. Viney, T.P. Russell, L.E. Depero. and R.J. Twieg, *Mol. Cryst, Liq. Cryst.,* **168,** 63 (1989).
[8] C. Viney, R.J. Twieg. T.P. Russell, and L.E. Depero. *Liq. Cryst.,* **5,** 1783 (1989).
[9] A. Bondi. *J. Phys. Chem.,* **68,** 441 (1964).
[10] G.D. Smith, R.L. Jaffe, and D.Y. Yoon, *Macromolecules,* **27,** 3166 (1994).